

See discussions, stats, and author profiles for this publication at: <https://www.researchgate.net/publication/231402060>

Kinetics and mechanisms of the reactions of methylthio, methylsulfinyl, and methyldithio radicals with ozone at 300 K and low pressures

ARTICLE *in* THE JOURNAL OF PHYSICAL CHEMISTRY · MARCH 1992

Impact Factor: 2.78 · DOI: 10.1021/j100184a027

CITATIONS

22

READS

12

3 AUTHORS, INCLUDING:



Florent Domine

Laval University

155 PUBLICATIONS 3,936 CITATIONS

SEE PROFILE



A.R. Ravishankara

Colorado State University

508 PUBLICATIONS 18,340 CITATIONS

SEE PROFILE

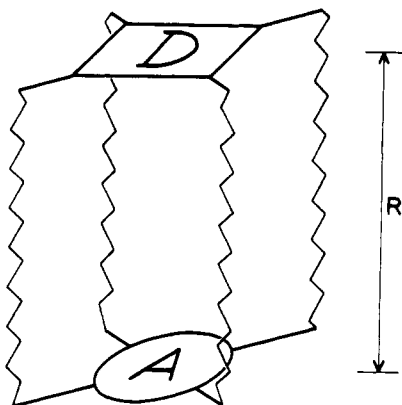


Figure 9. Schematic view of constrained donor-acceptor complex.

clear that the famous Thouless conditions¹⁶ are decisive when the symmetry-breaking takes the form of a bifurcation, but are not very useful when multistability is concerned.

B. Possible Guidelines for Bistability Conditions in DA Complexes. The model study of a DA complex ($\text{Li}_2 \cdots \text{F}$) was purely academic since it would lead to a strongly bound complex. A stable DA system should first involve a rigid chemical structure, i.e., chemical bonds maintaining the D and A partners at the appropriate intersystem distance R such that $R^{-1} \simeq \text{IP}(\text{D}) - \text{EA}(\text{A})$ (see Figure 9).

R should be large enough so that

$$|h| = |\langle \text{homo}_D | F | \text{lumo}_A \rangle_R| = \langle (\text{IP} - \text{EA})^{\text{vert}} - (\text{IP} - \text{EA})^{\text{adiab}} = 4\Delta E$$

The h integral may be rather small, even for relatively small R distances, if the highest occupied MO (homo) of D and lowest empty MO (lumo) of A are of different spatial symmetries.

Of course, these desires are somewhat contradictory. The ionization potential of conjugated molecules decreases with the size of the π system (8.15 eV for naphthalene, 7.04 eV for tetracene for instance²¹), but the difference between vertical and adiabatic ionization potentials also decreases with that size. The quantity $\text{IP}^{\text{vert}} - \text{IP}^{\text{adiab}}$ is only 0.10 eV for naphthalene and falls to 0.04 eV in tetracene.²² The use of properly substituted (conjugated) molecules should be considered to solve the conflict between the smallness of $\text{IP} - \text{EA}$ and the amplitude of $\Delta(\text{IP} - \text{EA})^{\text{vert-adiab}}$. Work is in progress in that direction, considering the (D,A) molecular pairs which organic conductors are built of, and for the localization of which the condition $2\Delta E > h$ was proposed by Shaik and Whangbo.²³

Registry No. H_4^+ , 12184-94-0; LiF, 7789-24-4; Li_2 , 14452-59-6; F, 14762-94-8; HF, 7664-39-3.

(21) Boschi, R.; Clar, E.; Schmidt, W. *J. Chem. Phys.* **1974**, *60*, 4406.

(22) Treboux, G., private communication.

(23) Shaik, S.; Whangbo, M. *Inorg. Chem.* **1986**, *25*, 9201.

Kinetics and Mechanisms of the Reactions of CH_3S , CH_3SO , and CH_3SS with O_3 at 300 K and Low Pressures

Florent Dominé, A. R. Ravishankara, and Carleton J. Howard*

National Oceanic and Atmospheric Administration, ERL, R/E/AL2, 325 Broadway, Boulder, Colorado 80303, and the Cooperative Institute for Research in Environmental Sciences, University of Colorado, Boulder, Colorado (Received: July 19, 1991; In Final Form: October 30, 1991)

The reactions of $\text{CH}_3\text{S} + \text{O}_3 \rightarrow \text{products}$ (1), $\text{CH}_3\text{SO} + \text{O}_3 \rightarrow \text{products}$ (2), and $\text{CH}_3\text{SS} + \text{O}_3 \rightarrow \text{products}$ (3) were investigated at 300 K in a discharge flow tube reactor coupled to a photoionization mass spectrometer. The measured value of k_1 is $(5.7 \pm 1.4) \times 10^{-12} \text{ cm}^3 \text{ molecule}^{-1} \text{ s}^{-1}$ in 1 Torr He. We observed that OH was produced in this reaction or in subsequent steps and that complex branched chain reactions, which generate CH_3S from its precursor molecule, took place in our flow tube reactor. We found that CH_3SO was a product of reaction 1 and the branching ratio for this channel was $15 \pm 4\%$, between 0.7 and 2.2 Torr He, independent of pressure. A preliminary value of $k_2 = (6 \pm 3) \times 10^{-13} \text{ cm}^3 \text{ molecule}^{-1} \text{ s}^{-1}$ was measured. CH_3S was not a major product of reaction 2. These results suggest that the reaction with O_3 is a major CH_3S removal process in the atmosphere. The rate coefficient for the reaction of CH_3SS with O_3 (3) was measured to be $k_3 = (4.6 \pm 1.1) \times 10^{-13} \text{ cm}^3 \text{ molecule}^{-1} \text{ s}^{-1}$.

Introduction

Dimethyl sulfide (CH_3SCH_3 , DMS) is estimated to make up between 50 and 90% of the total biogenic sulfur released to the atmosphere.¹ The CH_3S radical is thought to be an important intermediate in the atmospheric oxidation of DMS and of other biogenic sulfur compounds, such as methanethiol (CH_3SH) and dimethyl disulfide (CH_3SSCH_3 , DMDS).²⁻⁴ Therefore, several groups have investigated the reactions of CH_3S with the abundant tropospheric oxidants O_2 , NO_2 , and O_3 .⁵⁻⁹ Three groups have reported rate coefficients for the reaction of CH_3S with NO_2 ⁵⁻⁷ and obtained results in the range $(5-11) \times 10^{-11} \text{ cm}^3 \text{ molecule}^{-1} \text{ s}^{-1}$. Even though this reaction is fast, there generally is not enough NO_2 in the marine troposphere, where most of the DMS, and hence CH_3S , is present, to make this reaction an important CH_3S

removal. An earlier measurement suggested that the reaction of O_3 with CH_3S was slow⁸ $\leq 8 \times 10^{-14} \text{ cm}^3 \text{ molecule}^{-1} \text{ s}^{-1}$. The reaction of CH_3S with O_2 is very slow and an upper limit has been

(1) Andreae, M. O. In *The Biogeochemical Cycling of Sulfur and Nitrogen in the Remote Atmosphere*; Galloway, J. N., et al. Eds.; D. Reidel: Dordrecht, 1985; pp 5-25.

(2) Niki, H.; Maker, P. D.; Savage, C. M.; Breitenbach, L. P. *Int. J. Chem. Kinet.* **1983**, *15*, 647.

(3) Hatakeyama, S.; Akimoto, H. *J. Phys. Chem.* **1983**, *87*, 2387.

(4) Grosjean, D. *Environ. Sci. Technol.* **1984**, *18*, 460.

(5) Balla, R. J.; Nelson, H. H.; McDonald, J. R. *Chem. Phys.* **1986**, *109*, 101.

(6) Tyndall, G. S.; Ravishankara, A. R. *J. Phys. Chem.* **1989**, *93*, 2426.

(7) Dominé, F.; Murrells, T. P.; Howard, C. J. *J. Phys. Chem.* **1990**, *94*, 5839.

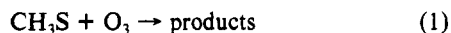
(8) Black, G.; Jusinski, L. E. *J. Chem. Soc., Faraday Trans. 2* **1986**, *82*, 2143.

(9) Tyndall, G. S.; Ravishankara, A. R. *J. Phys. Chem.* **1989**, *93*, 4707.

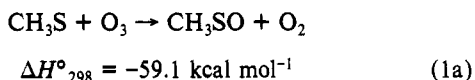
* Author to whom correspondence should be addressed at NOAA.

placed on its rate coefficient: $k \leq 2.5 \times 10^{-18} \text{ cm}^3 \text{ molecule}^{-1} \text{ s}^{-1}$.⁶ It is therefore uncertain as to what species or processes remove CH_3S from the atmosphere.

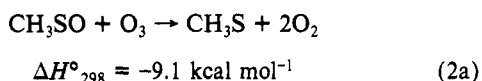
Recently, measurements by Tyndall and Ravishankara⁹ showed that the CH_3S reaction with O_3



was fast with $k_1 = (4.1 \pm 2.0) \times 10^{-12} \text{ cm}^3 \text{ molecule}^{-1} \text{ s}^{-1}$. However, some aspects of the $\text{CH}_3\text{S}/\text{O}_3$ chemistry still need to be clarified before the atmospheric importance of this reaction can be fully understood. Tyndall and Ravishankara observed regeneration of CH_3S but could not identify the chemistry responsible for it in their pulsed photolysis laser-induced fluorescence experiment. Based on the analogous $\text{HS}/\text{HSO} + \text{O}_3$ reaction mechanism,^{10,11} they suggested that reaction 1a could produce CH_3SO



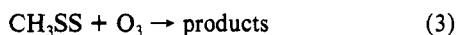
which may subsequently react with O_3 to regenerate CH_3S



The ΔH values for reactions 1a and 2a were obtained using heats of formation of 31 kcal mol^{-1} for CH_3S ¹² and 6 kcal mol^{-1} for CH_3SO .⁷ If this reaction scheme were correct, and if CH_3SO does not react with O_2 , reactions 1a and 2a will not result in a net loss of CH_3S . On the other hand, reaction 1 is fast enough to be the major atmospheric loss process for CH_3S , if the products of (1) were removed from the atmosphere without regenerating CH_3S in subsequent steps.

The objectives of the present study are (a) to examine the kinetics and mechanisms of the reactions of CH_3S and CH_3SO radicals with O_3 , (b) to determine what process or processes are responsible for the chain reactions observed by Tyndall and Ravishankara, and (c) to identify and quantify as many of the products and intermediates in the reaction scheme as possible. Our emphasis on the elucidation of the mechanism is facilitated by the use of a photoionization mass spectrometer which is capable of detecting many of the species we expect to be present in the reaction mixture, including CH_3 , CH_3S , CH_3SO , CH_2S , CH_3SS , and CH_3SSO .

The CH_3SS radical was formed by secondary chemistry in our source reactor and may be an intermediate in the atmospheric oxidation of DMDS. We have also measured the rate coefficient of its reaction with O_3

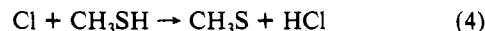


Experimental Section

The experimental system used in this study was a discharge flow tube with a photoionization mass spectrometer, which has been described previously.⁷ Therefore, it will not be described in detail here. The flow tube, with a 2.2 cm i.d., had a 50 cm long reaction region, and the average gas flow velocity, v , in the tube was approximately 2800 cm s^{-1} . All experiments were carried out under pseudo-first-order conditions, with the excess reactant, O_3 , added through a movable injector. The free radicals CH_3S , CH_3SO , and CH_3SS were produced in a side arm reactor. A fraction of the flow tube effluents were sampled into a differentially pumped ion source, where they were ionized by hydrogen Lyman α radiation (10.2 eV), obtained by flowing pure hydrogen at 0.6 Torr through a microwave discharge. The ions were then electrostatically focused into a second chamber, where they were mass selected with a quadrupole mass filter and detected by an electron multiplier.

During this study an accident occurred which damaged several components of the detection system. The rebuilt system suffered from increased background noise due to scattered UV light from the ion source. As a result, the detection limit for the present study was about $10^9 \text{ molecules cm}^{-3}$ for the sulfur compounds.

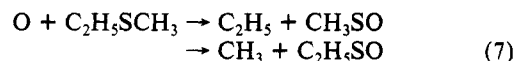
In this study, CH_3S radicals were produced by either of the following two reactions:



The source chemistry of these radicals has been described previously.⁷ It should be noted that the self-reaction of CH_3S produced DMDS, CH_2S , and CH_3SH , which are detectable in our system. The slower self-reaction of CH_3SO produces $\text{CH}_3\text{S}(\text{O})\text{S}(\text{O})\text{CH}_3$, CH_2SO , and CH_3SOH , which were also detected. Reaction 5 produced equal amounts of CH_3S and CH_3SO and was used to calibrate the response ratio of the instrument to CH_3S and CH_3SO , detected at masses 47 and 63. We found that the (mass 47)/(mass 63) signal ratio was 1.73. It was observed that CH_3SS was generated in the side arm reactor whenever CH_3S was produced. This was attributed⁷ to a heterogeneous reaction



which was used as a source of CH_3SS . We produced CH_3SO radicals by the reaction of ethyl methyl sulfide ($\text{C}_2\text{H}_5\text{SCH}_3$, EMS) with O atoms (7), as described previously⁷



We tested for the possibility of radical generation by reaction of the precursor gases with O_3 by turning off the microwave discharge and searching for radicals with the mass spectrometer. No detectable background signals were observed, indicating that no significant radical generation occurred when the source discharge was off.

The helium ($\geq 99.999\%$), hydrogen ($\geq 99.999\%$), oxygen ($\geq 99.97\%$), DMDS ($\geq 99\%$), EMS ($\geq 99\%$), and CCl_4 ($\geq 99.9\%$) were used without further purification. The CH_3SH ($\geq 99.5\%$) was purified by distillation. O_3 was stored on silica gel at 196 K and was eluted from the trap with a measured flow of He. The O_3 -He mixture then flowed through an absorption cell where the O_3 partial pressure was measured by the absorption at 254 nm, using a cross section of $1.15 \times 10^{-17} \text{ cm}^2 \text{ molecule}^{-1}$.¹³

Results

a. OH Production by the $\text{CH}_3\text{S}/\text{O}_3$ System. In the study of the $\text{CH}_3\text{S} + \text{O}_3$ reaction, CH_3S regeneration was observed. We have attempted to understand the chemistry responsible for this regeneration by using both reactions 4 and 5 as sources of CH_3S .

When CH_3S was produced by the reaction of Cl with CH_3SH (4), it was observed that in the presence of excess O_3 , the CH_3S signal showed an initial decay followed by an increase at longer reaction time, as shown in Figure 1. A signal at mass 63, assigned to CH_3SO produced by the reaction of CH_3S with O_3 , was also observed to increase with time. At a reaction time greater than 8 ms, with $[\text{O}_3] = 2.2 \times 10^{14} \text{ molecules cm}^{-3}$, the sum of the concentrations of CH_3S and CH_3SO was greater than the initial concentration of CH_3S . Since the first-order-order wall loss rate coefficients of CH_3S and CH_3SO are about 6 s^{-1} , these reactions can be neglected. This observation shows that the number of radicals in our reactor increases with time and that some complex chemistry with one or more branched chain reactions is taking place.

We suspected that OH might be involved in the chain branching. However, OH cannot be directly detected in our apparatus because its ionization potential is higher than the Lyman α energy, 10.2 eV. Therefore we added $\text{C}_2\text{F}_3\text{Cl}$, an efficient OH scavenger, to our reactor. The OH adds to $\text{C}_2\text{F}_3\text{Cl}$ with a rate coefficient of $6 \times 10^{-12} \text{ cm}^3 \text{ molecule}^{-1} \text{ s}^{-1}$ at 296 K in 1 Torr He.¹⁴

(10) Friedl, R. R.; Brune, W. H.; Anderson, J. G. *J. Phys. Chem.* **1985**, *89*, 5505.

(11) Wang, N. S.; Howard, C. J. *J. Phys. Chem.* **1990**, *94*, 8787.

(12) Shum, L. S. G.; Benson, S. W. *Int. J. Chem. Kinet.* **1983**, *15*, 433.

(13) DeMore, W. B.; Raper, O. *J. Phys. Chem.* **1964**, *68*, 412.

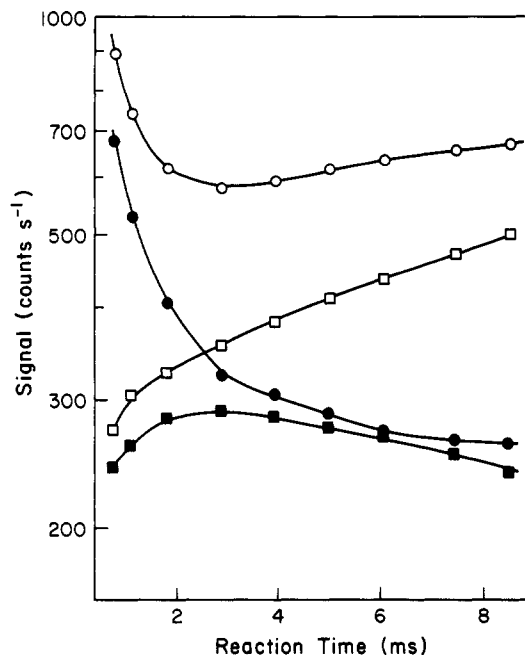


Figure 1. Plot of $[\text{CH}_3\text{S}]$ and $[\text{CH}_3\text{SO}]$ vs time, with $[\text{O}_3] = 2.2 \times 10^{14}$ molecule cm^{-3} ; source, $\text{Cl} + \text{CH}_3\text{SH}$, with $[\text{CH}_3\text{SH}] = 2.7 \times 10^{12}$ molecule cm^{-3} ; (○) CH_3S , (□) CH_3SO , with $[\text{C}_2\text{F}_3\text{Cl}] = 0$; (●) CH_3S , (■) CH_3SO , with $[\text{C}_2\text{F}_3\text{Cl}] = 2.3 \times 10^{14}$ molecules cm^{-3} .

We found that CH_3S , CH_3SS , and CH_3SO did not react with $\text{C}_2\text{F}_3\text{Cl}$ on the time scale of our experiments. As can be seen in Figure 1, in the presence of $\text{C}_2\text{F}_3\text{Cl}$ the CH_3S signal did not show any increase with reaction time, although the CH_3S decay plot was still nonexponential. The CH_3SO signal showed an initial increase followed by a decay, indicating that CH_3SO was a product of the O_3 and CH_3S reaction and that it reacted with O_3 . It also appears that in the presence of $\text{C}_2\text{F}_3\text{Cl}$ the sum of the concentrations of CH_3S and CH_3SO does not increase with reaction time.

The above observations are consistent with the following interpretation: (i) OH is formed in the reaction of CH_3S with O_3 or in some subsequent step. (ii) A branched chain reaction, which increases the number of radicals in the absence of $\text{C}_2\text{F}_3\text{Cl}$, takes place. (iii) OH reacts with CH_3SH to form CH_3S .⁹ (iv) In the presence of $\text{C}_2\text{F}_3\text{Cl}$, the first-order CH_3S decay plot shows some curvature, which is probably due mainly to the fragmentation of a heavier compound in the flow tube or in the ionization region, to give a CH_3S radical or a CH_3S^+ ion. This complication will be detailed later.

To test this interpretation, we used the $\text{O} + \text{DMDS}$ reaction as a source of CH_3S and CH_3SO . This source reaction eliminated the chlorine precursor and employed a different sulfur reagent. In the presence of O_3 , the CH_3S signal showed an initial decay followed by an increase as shown in Figure 2a. No initial decay was observed in the CH_3SO signal, which rose continuously over the time range investigated. A signal at mass 64 was observed to rise and was assigned to CH_3SOH , although we believe, as detailed below, that there is a minor contribution from S_2 . The rate of formation of CH_3SOH increased 5-fold between 3 and 18 ms. When $\text{C}_2\text{F}_3\text{Cl}$ was added to the flow tube, the CH_3S and CH_3SO signals were found to decrease with time, as shown in Figure 2b. The first-order decay of CH_3S was slightly curved, probably due to heavy compound fragmentation, while the decay of CH_3SO was exponential. Since the reaction of CH_3S with O_3 produces CH_3SO , some curvature in its decay might be expected. However, considering that the CH_3SO was formed mainly in the $\text{O} + \text{DMDS}$ source because the yield of CH_3SO from reaction 1 is small, as shown below, it is not surprising that a significant initial increase was not observed. The signal at mass 64 was found to decay with time and was much lower than when $\text{C}_2\text{F}_3\text{Cl}$ was absent.

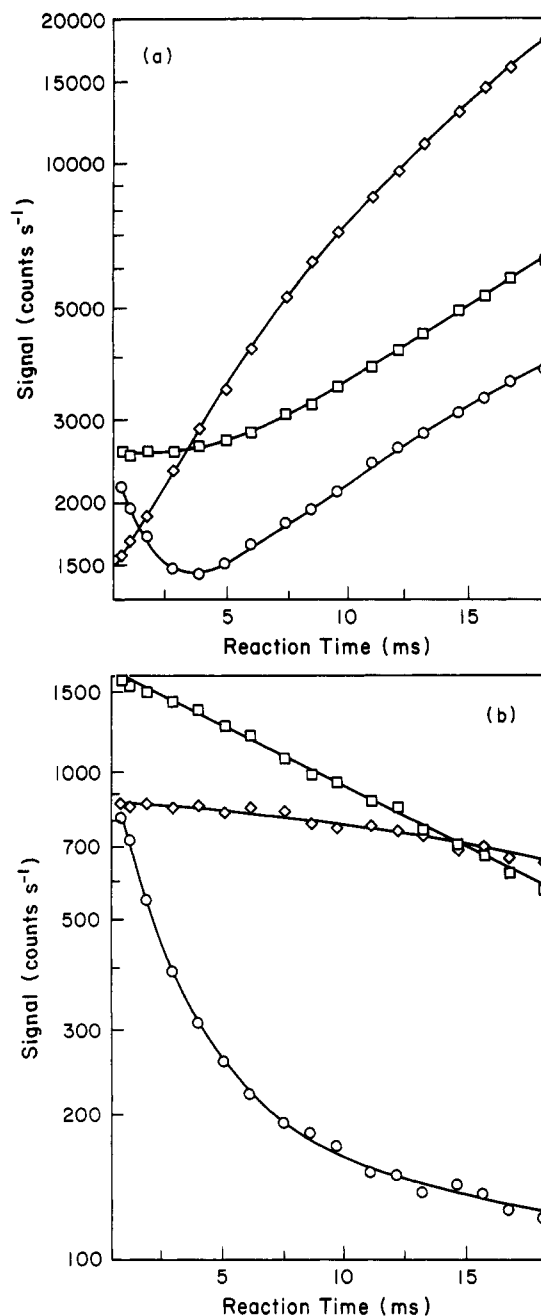
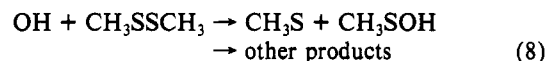


Figure 2. (a) Plot of $[\text{CH}_3\text{S}]$ (○), $[\text{CH}_3\text{SO}]$ (□), and $[\text{CH}_3\text{SOH}]$ (◇) vs time, with $[\text{O}_3] = 1.05 \times 10^{14}$ molecules cm^{-3} . Source was $\text{O} + \text{DMDS}$, with $[\text{DMDS}] = 1.6 \times 10^{12}$ molecules cm^{-3} . (b) Same as part a with $[\text{C}_2\text{F}_3\text{Cl}] = 1.02 \times 10^{15}$ molecules cm^{-3} added to the flow tube. Note different scales on the ordinates in parts a and b.

These observations are consistent with interpretations i, ii, and iv above and with the occurrence of reaction 8

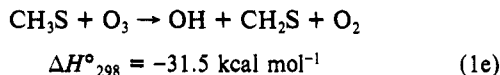


which generates CH_3S and CH_3SOH . In the presence of $\text{C}_2\text{F}_3\text{Cl}$, no CH_3SOH should be formed via reaction 8, although it is possible that some is made in the self-reaction of CH_3SO radicals to account for the residual signal observed at mass 64. Alternatively this signal may be due to S_2 . Since S_2 does not react with O_3 , $k < 4 \times 10^{-15} \text{ cm}^3 \text{ molecule}^{-1} \text{ s}^{-1}$,¹⁵ the decay of the mass 64 signal may be due to a reaction between the S_2 precursor and O_3 .

We have tried to understand the mechanism responsible for the formation of OH. Reaction 1e

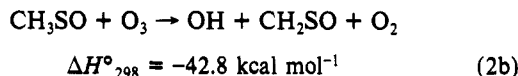
(14) Howard, C. J. *J. Chem. Phys.* 1976, 65, 4771.

(15) Hills, A. J.; Cicerone, R. J.; Calvert, J. G.; Birks, J. W. *J. Phys. Chem.* 1987, 91, 1199.



forms OH and could take place in our reactor. Since we cannot detect OH, this was tested by monitoring CH_2S at mass 46 in the presence of $\text{C}_2\text{F}_3\text{Cl}$. The fact that CH_2S is also formed in the source reactor by the self-reaction of CH_3S made this test difficult to perform. However, the CH_2S signals in the presence and in the absence of O_3 were the same, within the precision of our measurements. Assuming equal instrument responses for CH_2S and CH_3S , we conclude that the branching ratio for channel 1e is <4%. We believe that this assumption is reasonable, because we observed that the instrument response depended primarily upon the number of sulfur atoms in small organic species.⁷

Reactions involving some of the products of reaction 1 could also lead to the formation of OH. Reaction 2b



is a possibility that was investigated by monitoring the rise of CH_2SO product at mass 62. The ΔH value for reaction 2b was obtained using heats of formation of $-12 \text{ kcal mol}^{-1}$ for CH_2SO ¹⁶ and 6 kcal mol^{-1} for CH_3SO .⁷ Even though there are large uncertainties on both of these values, reaction 2b is definitely exothermic. To minimize interference from the $\text{CH}_3\text{S} + \text{O}_3$ chemistry, CH_3SO was produced by the reaction of EMS with O atoms (7). Figure 3a shows that, in the presence of O_3 , the mass 63 (CH_3SO) signal, after an initial decay, increased with reaction time to an intensity greater than the initial value. The mass 29 (C_2H_3) and mass 64 (CH_3SOH with a possible contribution from S_2) signals showed a similar pattern, while signals were observed to increase at masses 62 (CH_2SO) and 47 (CH_3S). In the presence of O_3 and $\text{C}_2\text{F}_3\text{Cl}$ (Figure 3b), the signals at masses 63, 29, and 64 showed nonexponential decays and the CH_3S and CH_2SO signals were observed to increase, although they did so more rapidly in the absence of $\text{C}_2\text{F}_3\text{Cl}$.

These observations are consistent with the following interpretation: (i) OH, CH_3S , and CH_2SO are formed when CH_3SO reacts with O_3 . The formation of CH_2SO suggests that OH may be formed in this reaction, although subsequent reactions also could also produce OH, or even CH_2SO . (ii) The increase in the number of radicals indicates that a branched chain reaction take place. (iii) OH reacts with EMS to regenerate C_2H_3 and produce CH_3SOH



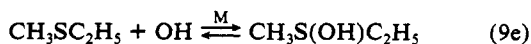
Other channels are possible for the reaction of EMS with OH. These include



$$\Delta H^\circ_{298} = -18 \text{ kcal mol}^{-1}$$



$$\Delta H^\circ_{298} = -9.3 \text{ kcal mol}^{-1}$$



$$\Delta H^\circ_{298} < 0$$

Heats of formation values of -14.3 and 31 kcal mol^{-1} have been used for EMS¹⁷ and CH_3S ,¹² respectively. The ΔH for reactions 9a, 9b, and 9e are not given because the heats of formation of CH_3SOH , $\text{C}_2\text{H}_3\text{SOH}$, and $\text{CH}_3\text{S}(\text{OH})\text{C}_2\text{H}_5$ are not known. The sulfur radical formed in reaction 9c will likely decompose to CH_3S and C_2H_4 (9d), as this process is endothermic by only about 9 kcal mol^{-1} . The adduct formation (9e) has been hypothesized by

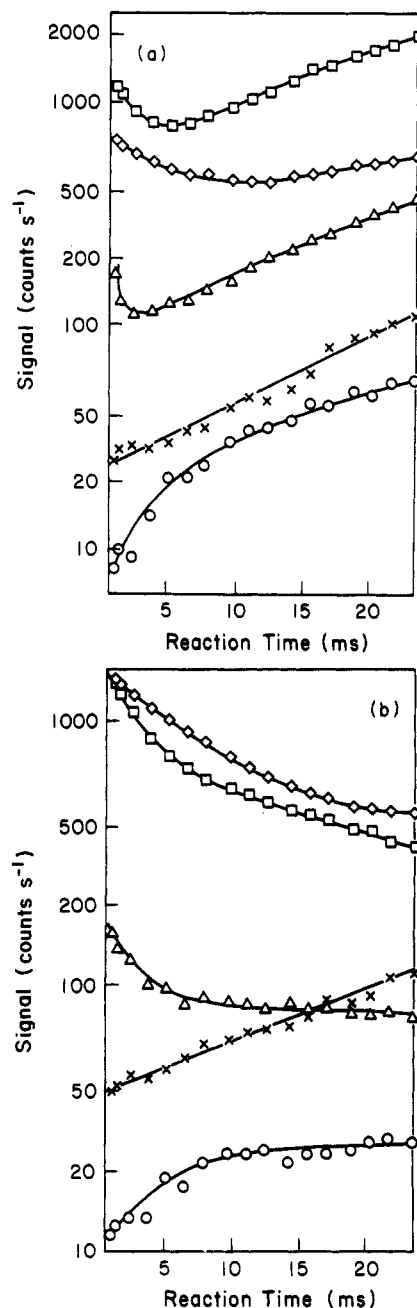


Figure 3. (a) Plot of $[\text{CH}_3\text{SO}]$ (\square), $[\text{CH}_3\text{SOH}]$ (\diamond), $[\text{C}_2\text{H}_3]$ (Δ), $[\text{CH}_2\text{SO}]$ (\times), and $[\text{CH}_3\text{S}]$ (\circ) vs time, with $\text{O}_3 = 3.0 \times 10^{14} \text{ molecules cm}^{-3}$. Source was $\text{O}/\text{C}_2\text{H}_5\text{SCH}_3$ with $[\text{C}_2\text{H}_5\text{SCH}_3] = 2.1 \times 10^{12} \text{ molecules cm}^{-3}$. (b) Same as part a with $[\text{C}_2\text{F}_3\text{Cl}] = 1.26 \times 10^{14} \text{ molecules cm}^{-3}$ added to the flow tube. Note different scales on the ordinates in parts a and b.

Hynes et al.¹⁸ and channels 9a and 9b correspond to the decomposition of the adduct. (iv) CH_3S reacts with O_3 to generate some CH_3SO . (v) In the presence of $\text{C}_2\text{F}_3\text{Cl}$ and O_3 , CH_3SO shows a nonexponential decay. This deviation from exponentiality is probably due to the fragmentation of heavier compounds to produce CH_3SO in the flow tube or to produce CH_3SO^+ ions in the ionization region. The decay of the mass 64 signal may be explained by reaction of the S_2 precursor with O_3 , while no CH_3SOH is being formed.

In summary, we have identified the reaction of CH_3SO with O_3 to be a possible source of OH. However, this chemical system is very complex and there may be other sources of OH. The branched chain reaction has not been identified but some possibilities are suggested in the discussion section.

(16) Benson, S. W. *Chem. Rev.* **1978**, *78*, 23.

(17) Stull, D. R.; Westrum, E. F., Jr.; Sinke, G. C. *The Chemical Thermodynamics of Organic Compounds*; John Wiley & Sons: New York, 1969; p 564.

(18) Hynes, A. J.; Wine, P. H.; Semmes, D. H. *J. Phys. Chem.* **1986**, *90*, 4148.

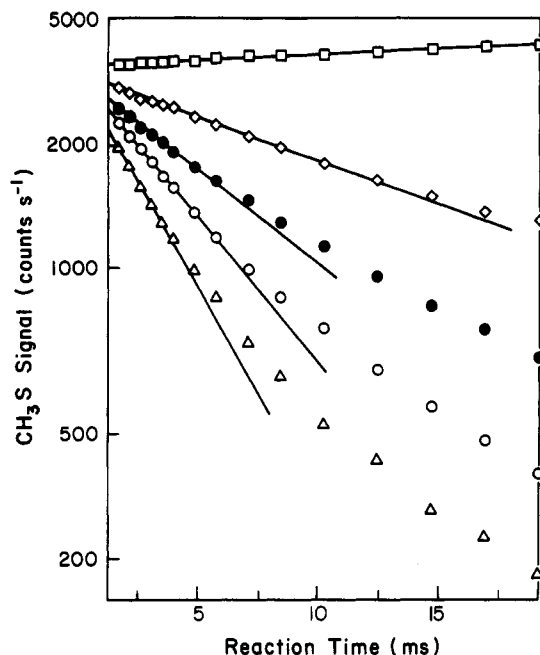


Figure 4. CH₃S + O₃ decay plots: source, Cl + CH₃SH; $T = 300 \pm 1$ K; $P = 1$ Torr; $v = 2850$ cm s⁻¹; [O₃] (10¹³ molecules cm⁻³) = 0 (□), 0.96 (◇), 2.01 (●), 3.44 (○), 5.48 (△).

b. Measurement of the Rate Coefficients of the Reactions of CH₃S and CH₃SS with O₃. To measure the rate coefficient of the reaction of CH₃S with O₃ at 300 K and 1 Torr, CH₃S radicals were produced in the side arm reactor by the reaction of Cl atoms with CH₃SH. Assuming similar instrument responses to CH₃SH and CH₃S, the initial concentrations of CH₃S used in the flow tube were estimated to be between 2×10^{10} and 5×10^{10} molecule cm⁻³. The decays of CH₃S in the presence of O₃ were measured under pseudo-first-order conditions in CH₃S. The [CH₃SH] was about 2×10^{12} molecules cm⁻³, while [C₂F₃Cl] was about 3×10^{14} molecules cm⁻³. This ensured that OH was effectively scavenged by C₂F₃Cl and thus that the regeneration of CH₃S by the reaction of OH with CH₃SH was suppressed. The plots of log (CH₃S signal at mass 47) vs time, shown in Figure 4, showed an initial linear decay followed by a curved decay. Such a curvature could be due to the regeneration of CH₃S by reactions other than by OH with CH₃SH. Indeed, Tyndall and Ravishankara⁹ observed the regeneration of CH₃S in their flash-photolysis laser-induced fluorescence study of the CH₃S + O₃ reaction. They suggested that this reaction produced CH₃SO with a yield of unity and that CH₃SO reacted with O₃ to regenerate CH₃S, also with a yield of unity. However, as detailed in the discussion section, the regeneration of CH₃S by these reactions is not large enough (about 2%) to explain the curvature shown in Figure 4. Another possible explanation would be that CH₃SH reacts with O₃, leading to a substantial loss of [O₃] in the reaction zone. However, since the [CH₃SH] was always much smaller than the [O₃], a substantial decrease in [O₃] due to such a reaction is unlikely, unless a chain reaction takes place. Moreover, we searched for, but did not detect, any reaction between CH₃SH and O₃ in our flow tube, and we place an upper limit of 1×10^{-15} cm³ molecule⁻¹ s⁻¹ on its rate coefficient. These possibilities being eliminated, we believe that the curvature shown in Figure 4 can be explained by a set of reactions similar to those described in our study of the CH₃S + NO₂ reaction.⁷ In that study CH₃SS was produced in the CH₃S source. The CH₃SS reacted with NO₂ to produce CH₃SSO, which was dissociatively ionized by Lyman α radiation in the ionization region to yield a CH₃S⁺ fragment. This fragment was detected at mass 47, thus interfering with the detection of CH₃S. As shown below, CH₃SS also reacts with O₃ and it is likely that CH₃SSO is a product of this reaction



The fragmentation of CH₃SSO in the ionization region would then

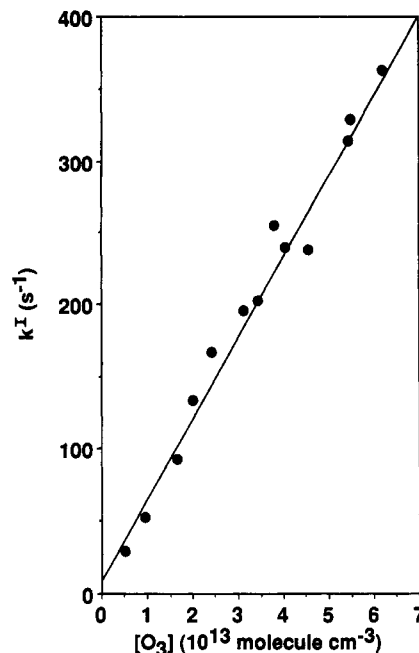
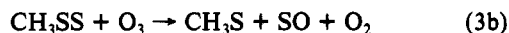


Figure 5. Plot of k^1 versus [O₃] for the CH₃S + O₃ reaction data: $T = 300 \pm 1$ K; $P = 1$ Torr; slope = 5.7×10^{-12} cm³ molecule⁻¹ s⁻¹.

result in the curvature observed on the plots of Figure 4. The CH₃S radical may also be a direct product of the CH₃SS reaction with O₃



$$\Delta H^\circ_{298} = -19.2 \text{ kcal mol}^{-1}$$

In our study of the CH₃S + NO₂ reaction, the curved decay plots were corrected by subtracting the contribution of the CH₃SSO fragmentation from the CH₃S⁺ signal. The resulting decay plots were exponential. However, taking the initial slopes of the curved plots or the slopes of the corrected decay plots gave first-order rate constant values different by less than 2%, which showed that such a correction was not essential. In the present case, the initial slopes of the decay plots were taken as a measurement of the first-order rate coefficients, k^1 .

A plot of k^1 versus [O₃] is shown in Figure 5, and its slope yields the second-order rate coefficient for reaction 1: $k_1 = (5.74 \pm 0.25) \times 10^{-12}$ cm³ molecule⁻¹ s⁻¹ with an intercept of 8 ± 9 s⁻¹, which is not statistically significant. The error limits are 1 σ based on precision only. Using uncertainties at the 95% confidence level for the gas flow rates ($\pm 3\%$), temperature ($\pm 1\%$), pressure ($\pm 1\%$), and flow tube radius ($\pm 1\%$) and taking into account an estimate of systematic errors which include errors due to the decay plots curvature, we suggest, $k_1 = (5.7 \pm 1.4) \times 10^{-12}$ cm³ molecule⁻¹ s⁻¹.

The CH₃SS radical was generated in our source whenever the CH₃S radical was produced. We believe that CH₃SS was formed by the reaction of CH₃S with elemental sulfur deposited on the walls of the source reactor. It is possible that some CH₃SS was also generated by this reaction taking place on the flow tube walls. However, this source of CH₃SS is probably negligible in the reaction zone because both the S and CH₃S react rapidly with O₃. To measure k_3 , the rate coefficient of the CH₃SS reaction with O₃, the decay of CH₃SS was measured in the presence of O₃ under conditions similar to those used for CH₃S. The decay plots were linear and their least-squares slopes gave the first-order rate coefficient of reaction 3. The plot of the first-order rate coefficient vs [O₃] is shown in Figure 6 and yields $k_3 = (4.63 \pm 0.12) \times 10^{-13}$ cm³ molecule⁻¹ s⁻¹ with an intercept 5 ± 3 s⁻¹. The error limits are 1 σ based on precision only. With an estimate of the total errors similar to that detailed for k_1 , we obtain $k_3 = (4.6 \pm 1.1) \times 10^{-13}$ cm³ molecule⁻¹ s⁻¹ at the 95% confidence level.

c. Yield of CH₃SO from the CH₃S + O₃ Reaction. The following procedures were used to measure the yield of CH₃SO from

TABLE I: CH₃SO Yield from the CH₃S + O₃ Reaction

pressure, Torr	[O ₃], 10 ¹⁴ molecules cm ⁻³	[CH ₃ SO] _{max} / [CH ₃ S] ₀ e ^{-(k_w+k_i)L/v}	t _{max} , ms		CH ₃ SO yield
			calcd	measd	
0.703	1.59	0.133	2.84	3.26	0.170
1.014	1.41	0.110	3.22	2.95	0.141
1.277	1.62	0.124	2.79	2.88	0.159
1.292	1.45	0.110	3.13	2.84	0.141
2.184	0.623	0.108	7.58	7.06	0.135
2.193	1.29	0.094	3.53	4.11	0.120
2.194	1.14	0.117	3.95	4.32	0.149
2.200	1.62	0.133	2.79	2.77	0.171
					0.15 ± 0.04 ^a

^a Average. Error is 95% confidence limit including an estimate for systematic error.

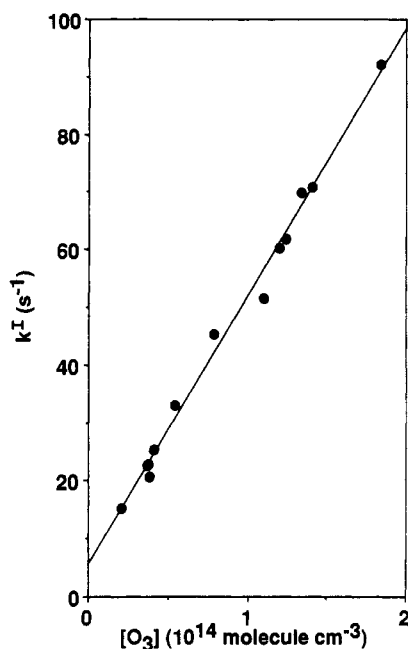
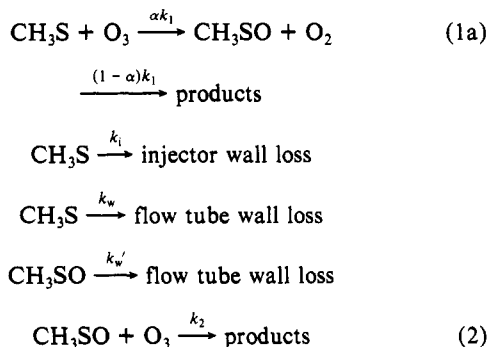


Figure 6. Plot of k^1 versus $[O_3]$ for the CH₃SS + O₃ reaction data: $T = 300 \pm 1$ K; $P = 1$ Torr; slope = 4.6×10^{-13} cm³ molecule⁻¹ s⁻¹.

reaction 1: (1) the temporal profiles of CH₃S and CH₃SO were measured; (2) a rate equation describing the temporal variations of [CH₃SO] was derived; (3) the rate constants of the reactions of CH₃SO with O₃ and of the wall losses of CH₃S and CH₃SO were measured; (4) these measured values, the measured value of k_1 , and the response ratios of the instrument to CH₃S and CH₃SO were used to fit the rate equation to obtain the yield of CH₃SO.

CH₃S radicals were produced by the Cl + CH₃SH reaction in the side arm reactor and reacted with O₃ in the flow tube in the presence of C₂F₃Cl, and the temporal profiles of CH₃S and CH₃SO were measured. The [CH₃SH] and [C₂F₃Cl] used were similar to those used for the measurement of k_1 . We assumed the following reaction sequence to define the CH₃SO temporal profile:



The regeneration of CH₃S by reaction 2 is neglected, as will be

justified later. The following integrated rate equation gives the concentration of CH₃SO

$$\begin{aligned}
 [\text{CH}_3\text{SO}] = & \frac{\alpha k_1 [\text{CH}_3\text{S}]_0 [\text{O}_3] e^{-(k_w+k_i)L/v}}{k_1 [\text{O}_3] - k_2 [\text{O}_3] - k_w' + k_w} (e^{-(k_2 [\text{O}_3] + k_w' - k_w - k_i)t} - e^{-(k_1 [\text{O}_3] - k_i)t}) \quad (10)
 \end{aligned}$$

The parameters of eq 10 are defined as follows: [CH₃S]₀, concentration of CH₃S, where the side arm reactor and the flow tube intersect; d , length of the reaction region, where O₃ and CH₃S are in contact; L , distance between the end of the flow tube and the side arm reactor; v , average flow velocity in the flow tube, assuming that v is not changed by the presence of the injector; t : reaction time between CH₃S and O₃. $t = d/v$. The quantity [CH₃S]₀e^{-(k_w+k_i)L/v} was measured independently, at [O₃] = 0 and with $d = 0$. The k_i was measured by flowing CH₃S in the absence of O₃ and monitoring the CH₃S signal as a function of injector position; a value of 6 s⁻¹ was found. Since the flow tube and the injector were both coated with halocarbon wax, we assumed that the surface loss of CH₃S was proportional to the surface area and we calculated $k_w = 17$ s⁻¹ based on the measured value of k_i . Similarly, by producing CH₃SO by reaction 7 and measuring its injector loss, we obtain $k_w' = 17$ s⁻¹. We need the value of k_2 to obtain α from eq 10. A few measurements made using reaction 7 as a source of CH₃SO yielded $k_2 = (6.0 \pm 3.0) \times 10^{-13}$ cm³ molecule⁻¹ s⁻¹, where the large error limit reflects the small number of measurements. A sensitivity analysis performed by using k_2 values of (6 and 3) $\times 10^{-13}$ in eq 10 showed that a 50% change in k_2 results in a change of only 6.5% in α , so a very accurate value of k_2 is not critical.

As expected, the plot of ln (CH₃SO signal) versus t showed a maximum, [CH₃SO]_{max}, which, according to eq 10, occurred at t_{max} given by

$$t_{\text{max}} = \frac{\ln(k_1 [\text{O}_3] - k_i) - \ln(k_2 [\text{O}_3] + k_w' - k_w - k_i)}{k_1 [\text{O}_3] + k_w - k_2 [\text{O}_3] - k_w'} \quad (11)$$

The time origin needed to determine the experimental values of t_{max} was taken as the point where the decay plots of Figure 4 intersect. The location of this point is consistent with the geometry of our flow tube reactor. Measured and calculated values of t_{max} are reported in Table I. Considering that the CH₃SO signal was measured only at discrete time intervals, the agreement between these two sets of values is reasonable.

Eight runs were performed at different pressures and O₃ concentrations. The yield of CH₃SO, $\alpha = k_{1a}/k_1$, was derived for each run by using the measured value of [CH₃SO]_{max} and the calculated value of t_{max} in eq 10. The calculated value, rather than the measured value, of t_{max} was used because [CH₃SO] was measured only at discrete time intervals. The data used for and obtained from these eight runs are reported in Table I. We find no systematic variation of the yield with pressure and we conclude that between 0.7 and 2.2 Torr He, α is independent of pressure. The average value of α is 15%, and with an estimate of various errors, we get $\alpha = 15 \pm 4\%$.

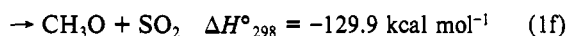
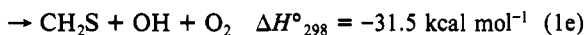
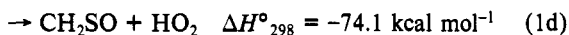
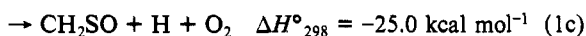
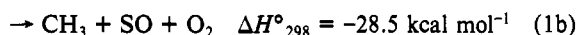
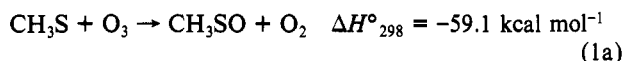
A few measurements of the yield of CH₃S from the CH₃SO + O₃ reaction were made in 1 Torr He, using reaction 7 as a source of CH₃SO. An analysis similar to the one described above was

performed, and the yield of CH₃S was found to be 13 ± 6%.

Discussion

The reaction of CH₃S with O₃ has previously been studied by Black and Jusinski⁸ and by Tyndall and Ravishankara.⁹ Black and Jusinski did not observe any reaction between CH₃S and O₃ in their flash-photolysis laser-induced fluorescence system and estimated $k_1 \leq 8 \times 10^{-14} \text{ cm}^3 \text{ molecule}^{-1} \text{ s}^{-1}$. However, it seems likely that under their experimental conditions, the regeneration of CH₃S was too fast to observe its decay, as pointed out by Tyndall and Ravishankara.⁹ Tyndall and Ravishankara used a system similar to Black and Jusinski and obtained $k_1 = (4.1 \pm 2.0) \times 10^{-12} \text{ cm}^3 \text{ molecule}^{-1} \text{ s}^{-1}$, which agrees with our value, within the quoted error limits. Tyndall and Ravishankara observed some CH₃S regeneration. To obtain the above value of k_1 , they performed a correction which assumed that CH₃SO from the CH₃S + O₃ reaction reacted with O₃ to give CH₃S with a yield of unity. Here we find that the yield of CH₃SO from the CH₃S + O₃ reaction is 15% independent of pressure between 0.7 and 2.2 Torr helium. Our preliminary results on the CH₃SO + O₃ reaction show that the yield of CH₃S from this reaction is 13 ± 6%. If the yields of CH₃SO and CH₃S from reactions 1 and 2 measured here at low pressure are valid at the pressures used by Tyndall and Ravishankara, 50–200 Torr He and 70–100 Torr SF₆, then the corrections made by these authors are unwarranted. The value of k_1 , that they measured without correction, $k_1 = 5.1 \times 10^{-12} \text{ cm}^3 \text{ molecule}^{-1} \text{ s}^{-1}$ would be the appropriate value. In that case, the agreement between their value and our value is very good.

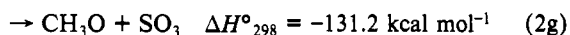
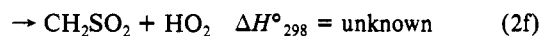
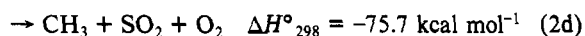
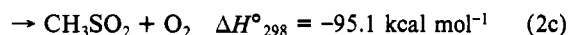
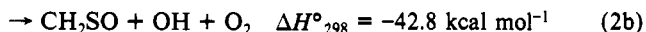
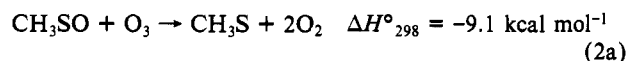
On the basis of known thermochemistry^{7,12,16} some of the possible channels for reaction 1 are shown in channels 1a–f.



Channels 1a and 1e have been investigated here. Although we observed signals at mass 15 (CH₃) and 62 (CH₂SO), we cannot quantify channels 1b, 1c, and 1d because, as shown below, CH₃ and CH₂SO could also be products of reaction 2. Moreover, CH₃ reacts rapidly with O₃,¹⁹ $k = 7 \times 10^{-13} \text{ cm}^3 \text{ molecule}^{-1} \text{ s}^{-1}$, and our detection limit for CH₃ is quite high (probably $> 5 \times 10^9$ molecules cm⁻³). We also cannot detect SO, produced in channel 1b. Channels 1a, 1b, and 1c are likely to be coupled. A large fraction of the 59 kcal mol⁻¹ energy from the highly exothermic channel 1a is likely to be deposited in the CH₃SO product. Indeed, the HSO product formed in the analogous HS + O₃ reaction^{10,11} is known to be highly excited.^{20,21} Since the bond dissociation energies $D(\text{CH}_3\text{--SO}) \approx 30 \text{ kcal mol}^{-1}$ and $D(\text{H--CH}_2\text{SO}) \approx 34 \text{ kcal mol}^{-1}$ are relatively small, these dissociation processes may be the major paths, particularly at low pressures. At higher pressures the excited CH₃SO may be substantially deactivated and the distribution of products may be quite different from our low pressure observations. Channel 1d involves a tight transition state and is probably slow. Channel 1e has been shown to be unimportant (<4%). This is not surprising because O₃ is expected to react at the radical site of the CH₃S. The reactions of HS and CH₃S with O₃ have similar rate constants, $k(\text{HS} + \text{O}_3) = 4.3 \times 10^{-12} \text{ cm}^3 \text{ molecule}^{-1} \text{ s}^{-1}$, and the reaction of HS with O₃ is known

to produce HSO.^{10,11} Reaction 1f seems unlikely, because it involves extensive rearrangement.

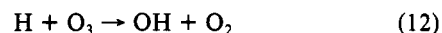
The products of the reaction of CH₃SO with O₃ are not all known. Some possibilities are given in channels 2a–g. Channel



2a has been identified here and we obtained a value of 13 ± 6% for the branching ratio of this channel. If we assume that the CH₂SO detected here is formed by reaction 2b and that our instrument responses to CH₃SO and CH₂SO are the same, the branching ratio for (2b) is 10%. However, channel 2b involves a hydrogen abstraction by ozone, and for reasons similar to those given above for reaction 1e, channel 2b seems to be an unlikely pathway. The CH₂SO detected in our reactor may come from reaction 1c, and CH₂SO would then be an important product of reaction 1. Regardless of its origin, CH₂SO is a new species that could be of atmospheric interest.

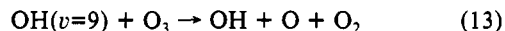
By analogy to the HS/HSO system^{10,11} and to the CH₃S + O₃ reaction, we expect reactions 2c, 2d, and 2e to be major routes. These channels are probably coupled. Reaction 2c is highly exothermic and a large fraction of this energy is probably deposited on the CH₃SO₂ product; therefore collisional deactivation of the energetic CH₃SO₂ product may affect the yields for channels 2c, 2d, and 2e. Reactions 2d and 2e represent the unimolecular dissociations of the energetic CH₃SO₂. Channel 2f, like reaction 1d, involves a tight transition state and is probably insignificant. Channel 2g involves extensive rearrangement and seems unlikely as an elementary reaction.

Since reactions 1e and 2b seem unlikely, the source of the OH present in our reactor is unclear. A likely possibility is that channel 1c and/or channel 2e is important. The H atoms produced in these reactions will then react rapidly, $k = 2.8 \times 10^{-11} \text{ cm}^3 \text{ molecule}^{-1} \text{ s}^{-1}$,²² to form OH



$$\Delta H^\circ_{298} = -76.9 \text{ kcal mol}^{-1}$$

The OH formed in this reaction is known to be vibrationally excited,²³ up to $v = 9$, and reacts rapidly with O₃, $k \approx 2 \times 10^{-10} \text{ cm}^3 \text{ molecule}^{-1} \text{ s}^{-1}$,²⁴ in a chain branching reaction²⁵



This reaction could be the chain branching reaction responsible for the increase in the number of radicals observed in our reactor. Both OH and O react with the sulfur radical precursors to regenerate CH₃S and/or CH₃SO.

The CH₃ produced in channels 1b and 2d might also be involved in a chain branching reaction. Washida et al.¹⁹ report that CH₃ reacts rapidly with O₃. A possible channel mentioned by these authors is



$$\Delta H = -148.5 \text{ kcal mol}^{-1}$$

(19) Washida, N.; Akimoto, H.; Okuda, M. *J. Chem. Phys.* **1980**, *73*, 1673.

(20) Schurath, U.; Weber, M.; Becker, K. H. *J. Chem. Phys.* **1977**, *67*, 110.

(21) Kendall, D. J. W.; O'Brien, J. J. A.; Sloan, J. J. *Chem. Phys. Lett.* **1984**, *110*, 183.

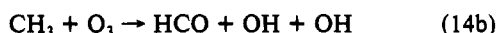
(22) Keyser, L. F. *J. Phys. Chem.* **1979**, *83*, 645.

(23) Polanyi, J. C.; Sloan, J. J. *Int. J. Chem. Kinet.* **1975**, *Symp. 1*, 51.

(24) Greenblatt, G. D.; Wiesenfeld, J. R. *J. Geophys. Res.* **1982**, *87*, 11145.

(25) Slinger, T. G.; Huestis, D. L. *Int. J. Chem. Kinet.* **1985**, *17*, 713.

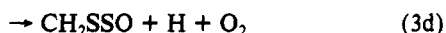
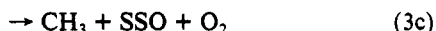
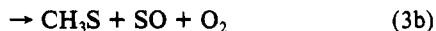
The HCOOH is probably formed highly excited, and we could also have



$$\Delta H = -41.9 \text{ kcal mol}^{-1}$$

Although this would help explain the observed OH generation, the amount of molecular rearrangement is formidable.

The rate coefficient for the reaction of CH₃SS with O₃ has not been reported previously. CH₃SS reacts with O₃ about 40 times slower than with NO₂.⁷ For CH₃S this ratio is about 10. Considering that the mechanisms of the CH₃S reactions with NO₂ and O₃ are an oxygen transfer,⁷ it is likely that an oxygen transfer is also involved in the CH₃SS + O₃ reaction



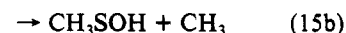
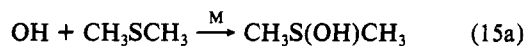
These four channels are probably coupled, in a manner, similar to that described for reactions 1 and 2. The production of CH₃S by channel 3b, and of CH₃SSO, which can be photodissociated by Lyman α radiation to CH₃S⁺ and SO,⁷ is consistent with the curvature of the CH₃S decay plots, in the presence of C₂F₃Cl.

Most of the products of reactions 1, 2, and 3 are still not accounted for. Further work is under way in our laboratory to elucidate this chemistry.

Atmospheric Implications. The fate of CH₃S radical in the atmosphere depends on the rates at which it reacts with different oxidizers, O₃, NO₂, and O₂. Using nominal mole fractions of 4×10^{-8} , 1×10^{-10} , and 0.21 for O₃, NO₂, and O₂ to represent conditions in the clean troposphere and the rate coefficients reported here and elsewhere^{6,7,9} for the CH₃S reactions, we estimate first-order rate coefficients of 6 s⁻¹, 0.15 s⁻¹, and ≤ 13 s⁻¹ for reactions of CH₃S with O₃, NO₂, and O₂. Tyndall and Ravishankara^{6,9} have suggested that the rate coefficient for the O₂ reaction is possibly an order of magnitude lower than the upper limit they derived. If this were the case, then the reaction with O₃ is the major loss process for CH₃S in the atmosphere, under most conditions. The results from our study show that, at low pressures, the regeneration of CH₃S in the O₃ reaction scheme is negligible, although it is possible that at atmospheric pressure the yield of CH₃SO is higher. Furthermore, the reaction of CH₃SO with O₂ could be enhanced in the atmosphere, if the CH₃SO formed by reaction 1 is excited. If the rate coefficient for the reaction of CH₃SO with O₂ is faster than even 1×10^{-19} cm³ molecule⁻¹ s⁻¹, the major loss process for CH₃SO would be reaction with O₂. Therefore, it is very likely that the reaction of CH₃S with O₃ leads to the loss of CH₃S from the atmosphere.

All the product information obtained here is strictly applicable to pressures lower than ~ 5 Torr. Although the yield of CH₃SO does not vary with pressure in the small range that was tested, our result may not be valid at pressures up to 760 Torr. The excited CH₃SO and CH₃SO₂ formed in the CH₃S + O₃ and CH₃SO + O₃ reactions may be quenched and stabilized in the atmosphere. However, if we assume that our observations are valid in the atmosphere, it is clear that the oxidation of CH₃S by O₃ primarily leads to cleavage of the C-S bond. For the formation of methanesulfonic acid (MSA, CH₃SO₃H) the CH₃S moiety must remain intact. This may explain the high yields of MSA from DMS oxidation found in the presence of NO_x.^{3,4} in chamber experiments. When CH₃S is oxidized by NO₂, we expect CH₃SO and CH₃SO₂ to be formed. These species may lead to formation of MSA. One possibility is that CH₃SO adds O₂ forming CH₃SO₃, which leads to MSA.²⁶ If the C-S bond is cleaved, oxidation of SO to SO₂ will be rapid.

Our observation of C₂H₅ and CH₃SOH in (9a), the reaction of OH and C₂H₅SCH₃, has some interesting implications. There is evidence that the reaction of OH with CH₃SCH₃ in the atmosphere²⁰ proceeds via either H atoms abstraction or OH addition to sulfur followed by reaction of the adduct with O₂.¹⁸ Hynes et al.¹⁸ have assessed the branching ratios for these channels by measuring the loss rate coefficient for OH under various conditions of temperature, pressure, and composition and by assuming a two-channel model. Our observation of C₂H₅ and CH₃SOH production indicates that the C-S bond may be cleaved by OH addition to CH₃SCH₃ as well



where a third body (M) may be involved in one or both of these steps. This reaction could appear as an abstraction, when OH loss is monitored. The interpretation of the kinetic isotope effect reported by Hynes et al. is complex, because the reaction has a negative activation energy and involves the formation of an adduct. Furthermore, if the OH reaction pathway does indeed cleave the C-S bond, it will require a reanalysis of the observed variation of the OH loss rate coefficient with pressure and O₂ composition. In any case, further studies on the OH reaction with DMS aimed at elucidating the mechanism are necessary.

Acknowledgment. This work was supported by NOAA as part of the National Acid Precipitation Assessment Program.

Registry No. CH₃S, 7175-75-9; CH₃SO, 25683-64-1; CH₃SS, 29245-72-5; O₃, 10028-15-6.

(26) Jensen, N. R.; Hjorth, J.; Lohse, C.; Skov, H.; Restelli, G. *J. Atmos. Chem.*, in press, and references cited therein.